ELSEVIER

Inorganic Chemistry Communications 5 (2002) 107–111

INORGANIC CHEMISTRY COMMUNICATIONS

www.elsevier.com/locate/inoche

^{57}Fe Mössbauer spectroscopic and X-ray structural analyses on the mixed-valence state of biferrocenium derivatives with bromoalkyl substituents

Teng-Yuan Dong [a,*], Ling-Shao Chang [a], Gene-Hsiang Lee [b], Shie-Ming Peng [b]

[a] *Department of Chemistry, National Sun Yat-Sen University, Kaohsiung, Taiwan*
[b] *Department of Chemistry, National Taiwan University, Taipei, Taiwan*

Received 20 August 2001; accepted 22 November 2001

Abstract

The mixed-valence states of biferrocenium triiodide salts with bromoalkyl substituents, have been investigated by means of ^{57}Fe Mössbauer spectroscopy and X-ray structural determinations. © 2002 Published by Elsevier Science B.V.

Keywords: Mixed-valence compound; Biferrocenium; Metallocene; Electron transfer

1. Introduction

The electronic interaction and the electron-transfer process between the two iron centers in the series of mixed-valence biferrocenium triiodide salts (**1**) have been extensively studied in understanding what factors influence the electronic structures of the iron sites [1–8] (Scheme 1).

The first strategy is the use of a series of the mixed-valence biferrocenium with short alkyl substituents (**1a**–**e**). In **1a**–**e**, the importance of the cation symmetry and its packing effect in the crystal structure has been shown [6]. The second strategy is the use of the mixed-valence biferrocenium salts with long alkyl substituents (**1e**–**o**) [2,4]. It has shown an even–odd character in the number of carbon atoms of the substituents in the relationship between the crystal structure and the mixed-valence state [4]. Compounds with 6-, 8-, 10-, 12-, 14-, and 16-carbons alkyl substituent give a temperature-dependent detrapped-valence state. However, it seems difficult to separate the contribution of the symmetry of the cation and the packing effect in the crystal. The third strategy is the use of the derivatives attached to a planar substituent (**1p**–**q**) [1,3,7,8]. In compounds **1p** and **1q**, there is a close connection between the mixed-valence state and the cation–cation interaction formed through the π–π interaction of the benzene ring. Our strategy for systematic design is to use derivatives (**2a**–**e**) with the terminal bromide in the alkyl substituent. If the symmetry of the cation and the intermolecular interactions (cation–cation and cation–anion interactions) are indeed important on the mixed-valence state, the terminal bromide in the alkyl substituent would play an important role.

2. Results and discussion

The corresponding neutral biferrocenes of **2a**–**e** were prepared (Chart 1) according to the Friedel–Crafts synthesis by mixing an equimolar amount of the acyl chloride and excess $AlCl_3$ in dried CH_2Cl_2 at 0 °C under N_2, and then followed a reduction reaction with $LiAlH_4/AlCl_3$ in dried ether. The triiodide salts were prepared according to the simple procedure previously reported for biferrocenium triiodide [1].

^{57}Fe Mössbauer spectra were run for **2a**–**d**. The 300 and 80 K Mössbauer spectra of the asymmetric biferrocenium **2a**–**c** show two doublets, Fe(II) and Fe(III) sites. This pattern is expected for a mixed-valence

---

[*] Corresponding author. Fax: +886-7-5253-908.
E-mail address: dty@mail.nsysu.edu.tw (T.-Y. Dong).

1387-7003/02/$ - see front matter © 2002 Published by Elsevier Science B.V.
PII: S1387-7003(01)00354-9

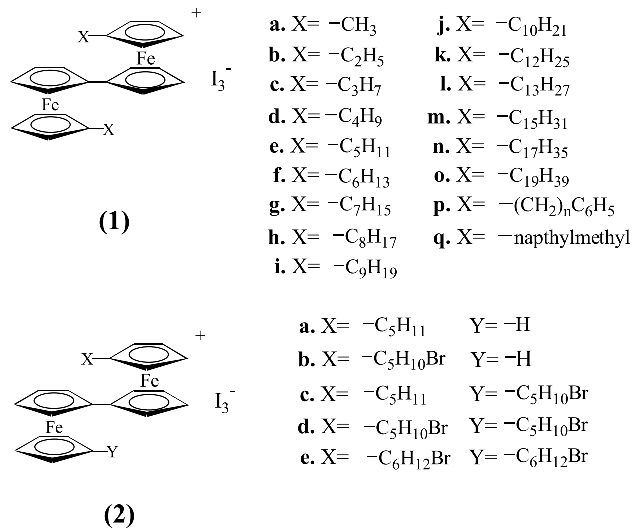

(1)

a. X= $-CH_3$
b. X= $-C_2H_5$
c. X= $-C_3H_7$
d. X= $-C_4H_9$
e. X= $-C_5H_{11}$
f. X= $-C_6H_{13}$
g. X= $-C_7H_{15}$
h. X= $-C_8H_{17}$
i. X= $-C_9H_{19}$
j. X= $-C_{10}H_{21}$
k. X= $-C_{12}H_{25}$
l. X= $-C_{13}H_{27}$
m. X= $-C_{15}H_{31}$
n. X= $-C_{17}H_{35}$
o. X= $-C_{19}H_{39}$
p. X= $-(CH_2)_nC_6H_5$
q. X= −napthylmethyl

(2)

a. X= $-C_5H_{11}$ Y= −H
b. X= $-C_5H_{10}Br$ Y= −H
c. X= $-C_5H_{11}$ Y= $-C_5H_{10}Br$
d. X= $-C_5H_{10}Br$ Y= $-C_5H_{10}Br$
e. X= $-C_6H_{12}Br$ Y= $-C_6H_{12}Br$

Scheme 1.

biferrocenium cation which is valence-trapped on the timescale of the Mössbauer technique ($\sim 10^7$ s^{-1}). It has been reported [9] that the decrease of the quadrupole splitting (ΔE_Q) in the ferrocenyl doublet (Fe(II) site) and the increase of the ΔE_Q in the ferrocenium doublet (Fe(III) site) are an indication of the magnitude of intramolecular electron transfer rate in the biferrocenium cation. At 300 K, the respective values of $\Delta\Delta E_Q$, which is the difference of ΔE_Q between Fe(II) and Fe(III) sites, for **2a**–**c** are 1.831, 1.815, 0.938 mm s^{-1}. Thus the order of the intramolecular electron-transfer rate is **2c** $>$ **2b** $\approx$ **2a**. Here, we suggest that the most important factor in controlling the rate of electron transfer is the symmetry of the cation. The cations of **2a**–**c** are asymmetric, that is, the two irons are not in equivalent environments. This asymmetry induces a nonzero zero-point energy barrier for electron transfer.

Compound **2c** serves as a very sensitive probe to sense the importance of the symmetry of the two Fe sites. It has been reported [9] that the magnitude of the zero-point energy difference can be estimated from the two one-electron oxidation waves of neutral biferrocene. A comparison of the magnitude of $\Delta E_{1/2}$ (the difference of two half-wave potentials) for the neutral 1,1′-dipentylbiferrocene ($\Delta E_{1/2} = 0.38(1)$ V), the neutral 1,1′-dibromopentylbiferrocene ($\Delta E_{1/2} = 0.38(1)$ V) and the neutral 1-pentyl-1′-(5-bromopentyl)biferrocene ($\Delta E_{1/2} = 0.39(1)$ V) indicates the zero-point energy difference between two vibronic states in asymmetrical biferrocenium cation **2c** is rather small, which is reasonable in terms of the small effect of the bromide substituent on the structure of the cation **2c** in the *solution* state. The cation **2c** has a Mössbauer-localized electronic structure in the *solid* state. However, the symmetric 1,1′-di(bromopentyl)biferrocenium is Mössbauer delocalized above 120 K as shown in Fig. 1. Hence it appears that the electrochemically unmeasureable zero-point energy difference plays a rather important role in determining the nature of electron transfer.

It is even more surprising that the cation in **2e** shows two doublets (valence-trapped, $\Delta E_Q = 0.492$ and 1.946 mm s^{-1}) in the 300 K Mössbauer spectrum. We believe that the most important factor in controlling the nature of electron transfer is the symmetry of the cation in the *solid* state. As shown in Fig. 2, further evidence can be gleaned from the single X-ray structural determinations of **1e**, **2d** and **2e**.

In **1e** and **2e**, the two metallocene moieties in the cation are not equivalent. The Fe–C distances and Fe–Cp distances are not equivalent. More significantly, the subsituent on the Cp ring is situated differently. In **1e** and **2e**, the average Fe1–C and Fe1–Cp distances indicate that the Fe1 is in the Fe(II) oxidation state. Fur-

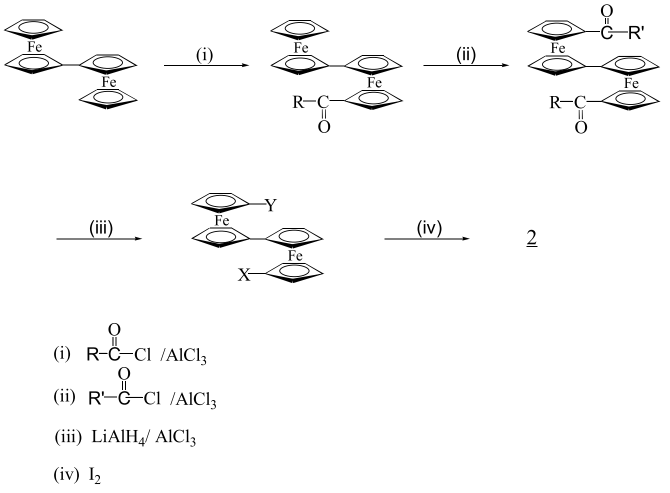

(i) $R-\overset{O}{\overset{\|}{C}}-Cl$ /$AlCl_3$
(ii) $R'-\overset{O}{\overset{\|}{C}}-Cl$ /$AlCl_3$
(iii) $LiAlH_4$/ $AlCl_3$
(iv) I_2

Chart 1.

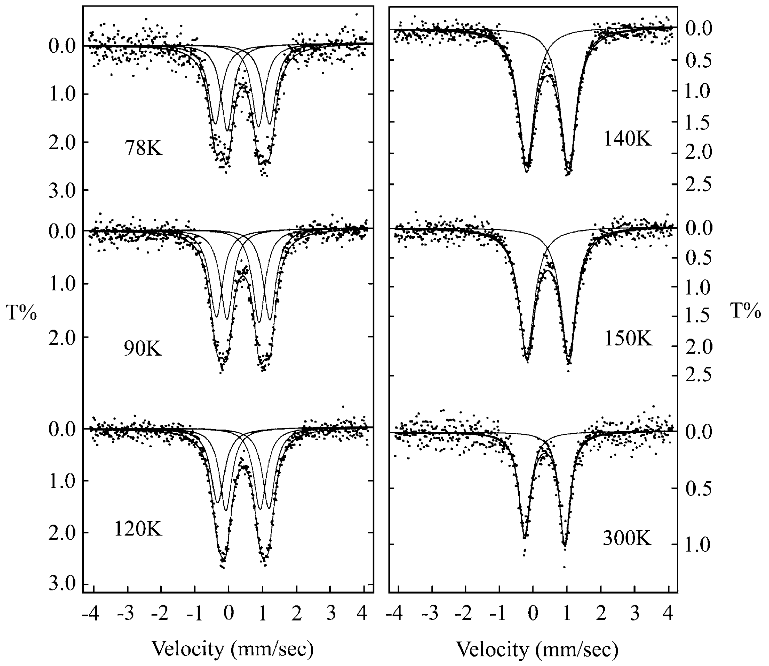

Fig. 1. ^{57}Fe variable-temperature Mössbauer spectra for **2d**.

thermore, the average Fe2–C and Fe2–Cp distances indicate that the Fe2 is in the Fe(III) oxidation state. In contrast to compounds **1e** and **2e**, the two metallocene moieties in the Mössbauer-delocalized cation **2d** are crystallographically equivalent. The refinement of the structure imposes inversion centers on both the cation and the triiodide anion. Therefore, the mixed-valence state in **2d** becomes valence detrapped. On the other hand, in asymmetric biferrocenium cations **1e** and **2e** the valence-trapped state is observed at room temperature.

3. Experimental

3.1. General information

All manipulations involving air-sensitive materials were carried out by standard Schlenk techniques under an atmosphere of N_2. Chromatography was performed on neutral alumina (Merck, act. II). The sample of biferrocene was prepared according to the literature procedure [10].

3.2. Acylation of biferrocene

The acylating reagent was made-up according to the Friedel–Crafts synthesis by mixing acyl chloride and excess $AlCl_3$ in dried CH_2Cl_2 for 20 min at 0 °C under N_2. The excess $AlCl_3$ was filtered out with glass wool. The acylating reagent was added by means of a dropping funnel over a period of about 1 h to a solution of biferrocene in dried CH_2Cl_2 at −78 °C. The reaction mixture was stirred for 6 h at −78 °C. The resulting mixture was separated after the reduction of ferrocenium ion with aqueous $Na_2S_2O_3$. The organic layer was washed with saturated aqueous $NaHCO_3$ and water and it was then dried over $MgSO_4$. The solvent was removed under reduced pressure. The red residue was chromatographed.

3.3. General reduction of acylbiferrocene

The reduction reaction was carried out by carefully adding, with stirring, small portions of $AlCl_3$ to a mixture of acylbiferrocene and $LiAlH_4$ in dried ether. After 40 min, an excess of H_2O was added to it, and the ether layer was separated. The ether layer was washed with water and dried over $MgSO_4$. After the evaporation of the solvent, the crude product was chromatographed. All new compounds gave satisfactory spectroscopic and analytical data. Selected physical data: for neutral **2a**: m.p. 81.5–82 °C; M^+; m/z 440; ^{1}H NMR (500 MHz, $CDCl_3$) δ 0.88 (t, 3H, CH_3), 1.21 (m, 2H, CH_2), 1.27 (m, 2H, CH_2), 1.39 (m, 2H, CH_2), 2.11 (t, 2H, CH_2), 3.85 (t, 2H, Cp), 3.89 (t, 2H, Cp), 3.99 (s, 5H, Cp), 4.12 (t, 2H, Cp), 4.17 (t, 2H, Cp), 4.26 (t, 2H, Cp), 4.35 (t, 2H, Cp). For neutral **2b**: m.p. 94.5–95.5 °C; M^+, m/z 518, 520; ^{1}H NMR (500 MHz, $CDCl_3$) δ 1.38 (m, 4H, CH_2), 1.82 (t, 2H, CH_2), 2.11 (t, 2H, CH_2), 3.38 (t, 2H, CH_2), 3.84 (t, 2H, Cp), 3.89 (t, 2H, Cp), 3.98 (s, 5H, Cp), 4.12 (t, 2H, Cp), 4.18 (t, 2H, Cp), 4.26 (t, 2H, Cp), 4.34 (t, 2H, Cp). For neutral **2c**: m.p. 34–36 °C; M^+, m/z 588, 590; ^{1}H NMR (500 MHz, $CDCl_3$) δ 0.87 (t, 3H, CH_3), 1.26 (m, 4H, CH_2), 1.38 (M, 4H, CH_2), 1.81 (t, 4H, CH_2), 2.09 (t,

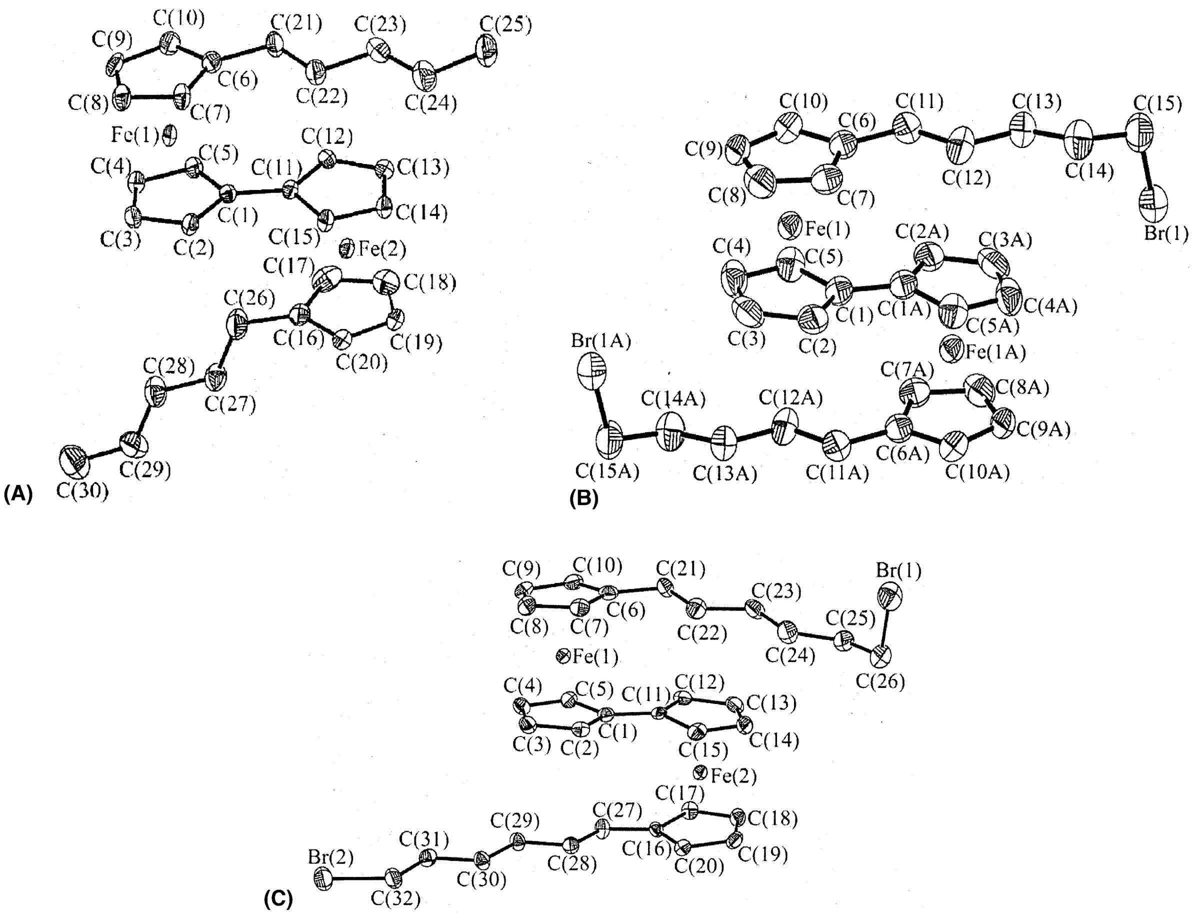

Fig. 2. Molecular structure and important bond lengths (Å) and bond angles (°) of (A) **1e**: aver. Fe1–C 2.056(5), aver. Fe2–C 2.086(5), I1–I2 2.9853(5), I1–I3 2.8721(5), I3–I2–I1 178.53(2), aver. Fe1–Cp 1.662, aver. Fe2–Cp 1.700, (B) **2d**: aver. Fe–C 2.060(5), I1–I2 2.916(1), I2–I1–I2 180.0, aver. Fe–Cp 1.672, and (C) **2e**: aver. Fe1–C 2.056, aver. Fe2–C 2.092, I1–I2 2.9305(5), I3–I4 2.9234(4), I2–I1–I2 180.0, I4–I3–I4 180.0, aver. Fe1–Cp 1.656, aver. Fe2–Cp 1.706.

4H, CH_2), 3.38 (t, 2H, CH_2), 3.83 (s, 4H, Cp), 3.88 (t, 4H, Cp), 4.12 (s, 4H, Cp), 4.24 (s, 4H, Cp). For neutral **2d**: m.p. 68.5–69.5 °C; M^+, m/z 666, 668, 670; ^1H NMR (500 MHz, $CDCl_3$) δ 1.37 (m, 8H, CH_2), 1.81 (t, 4H, CH_2), 2.09 (t, 4H, CH_2), 3.38 (t, 4H, CH_2), 3.83 (t, 4H, Cp), 3.89 (t, 4H, Cp), 4.13 (t, 4H, Cp), 4.24 (t, 4H, Cp). For neutral **2e**: m.p. 59.5–61 °C; M^+, m/z 695, 697, 699; ^1H NMR (500 MHz, $CDCl_3$) δ 1.24 (m, 4H, CH_2), 1.38 (m, 8H, CH_2), 1.83 (m, 4H, CH_2), 2.08 (t, 4H, CH_2), 3.40 (t, 4H, CH_2), 3.83 (t, 4H, Cp), 3.88 (t, 4H, Cp), 4.12 (t, 4H, Cp), 4.24 (t, 4H, Cp).

3.4. Mixed-valence compounds

Compounds were prepared according to the simple procedure previously reported for biferrocenium triiodide [1].

3.5. Physical methods

The ^{57}Fe Mössbauer spectra were run on a constant-acceleration instrument which has been previously described [11]. ^1H NMR spectra were run on a Varian VXR-300 spectrometer. Mass spectra were obtained with a VG-BLOTECH-QUATTRO 5022 system. Electrochemical measurements were carried out with a BAS 100 W system. Cyclic voltammetry was performed with a stationary Pt working electrode. These experiments were carried out with a 1×10^{-3} M solution of biferrocene in CH_2Cl_2/CH_3CN (1:1) containing 0.1 M of $(n\text{-}C_4H_9)_4NPF_6$ as a supporting electrolyte. The potentials quoted in this work are relative to a Ag/AgCl electrode at 25 °C.

The single-crystal X-ray determinations were carried out on an Enraf Nonius CAD4 diffractometer for **2d** and on a Siemens CCD diffractometer for **1e** and **2e**. Crystals data: for **1e**: $C_{30}H_{38}Fe_2I_3$, $M = 891.00$, $T = 150(1)$ K, monoclinic, space group $P2_1/c$, $a = 23.5809(3)$, $b = 9.4328(1)$, $c = 10.918(1)$ Å, $\beta = 96.913(1)°$, $U = 3092.25(6)$ Å^3, $F(000) = 1716$, $D_c = 1.914$ g cm^{-3}, $Z = 4$, $\mu = 3.950$ mm^{-1}, λ(Mo-Kα) = 0.71073 Å, $R1 = 0.0437$, $wR2 = 0.0823$. Intensity data were collected to a 2θ limit of 55°. Of the 18 973 reflections collected, there were 6929 with $F_0^2 > 2.0\sigma(F_0^2)$. For **2d**:

$C_{30}H_{36}Br_2Fe_2I_3$, $M = 1048.81$, $T = 295(2)$ K, triclinic, space group $P\bar{1}$, $a = 9.512(2)$, $b = 9.882(2)$, $c = 10.829(2)$ Å, $\alpha = 110.05(2)°$, $\beta = 114.22(2)°$, $\gamma = 98.98(2)°$, $U = 818.0(3)$ Å^3, $F(000) = 497$, $D_c = 2.129$ g cm^{-3}, $Z = 1$, $\mu = 6.178$ mm^{-1}, λ(Mo-Kα) = 0.71073 Å, $R1 = 0.0377$, $wR2 = 0.0927$. Intensity data were collected to a 2θ limit of 55°. Of the 2302 reflections collected, there were 3755 with $F_0^2 > 2.0\sigma(F_0^2)$. For **2e**: $C_{32}H_{40}Br_2Fe_2I_3$, $M = 1076.86$, $T = 150(1)$ K, triclinic, space group $P\bar{1}$, $a = 9.8734(1)$, $b = 10.4073(1)$, $c = 18.4792(3)$ Å, $\alpha = 80.924(1)°$, $\beta = 77.663(1)°$, $\gamma = 67.498(1)°$, $U = 1707.68(4)$ Å^3, $F(000) = 1026$, $D_c = 2.094$ g cm^{-3}, $Z = 2$, $\mu = 5.922$ mm^{-1}, λ(Mo-Kα) = 0.71073 Å, $R1 = 0.0446$, $wR2 = 0.1111$. Intensity data were collected to a 2θ limit of 55°. Of the 19 204 reflections collected, there were 7657 with $F_0^2 > 2.0\sigma(F_0^2)$. Absorption corrections were made with empirical φ rotation. The structure was solved from heavy-atom electron density maps and refined by full-matrix least squares analysis. All non-hydrogen atoms were refined anisotropically. During the final cycles of refinement fixed hydrogen contributions with C–H bond lengths fixed at 0.98 Å were applied.

4. Supplementary material

Tables of atomic, positional and thermal parameters, bond angles and distances. Crystallographic data for the structural analysis has been deposited with Cambridge Crystallographic Data Centre, CCDC 173144–173146. Copies of this information maybe obtained free of Charge from: The Director, CCDC, 12 Union Road, Cambridge, CB2 1EZ, UK (Fax: +44-1223-336033; email: deposit@ccdc.cam.ac.uk or www:http://www.ccdc.cam.ac.uk).

Acknowledgements

We thank the National Science Council (NSC89-2113-M-110-019) for support.

References

[1] T.-Y. Dong, P.H. Ho, X.Q. Lai, Z.W. Lin, K.J. Lin, Organometallic 19 (2000) 1096, and references therein.
[2] S. Nakashima, Y. Ueki, H. Sakai, J. Chem. Soc., Dalton Trans. (1995) 513.
[3] S. Nakashima, A. Hori, H. Sakai, M. Watanabe, I. Motoyama, J. Organomet. Chem. 542 (1997) 271.
[4] S. Nakashima, S. Nakazaki, H. Sakai, M. Watanabe, I. Motoyama, M. Sato, Inorg. Chem. 37 (1998) 1959.
[5] S. Nakashima, T. Oda, T. Okuda, M. Watanabe, Inorg. Chem. 38 (1999) 4005.
[6] T.-Y. Dong, D.N. Hendrickson, K. Iwai, M.J. Cohn, S.J. Geib, A.L. Rheingold, H. Sano, I. Motoyama, S. Nakashima, J. Am. Chem. Soc. 107 (1985) 7996.
[7] T.-Y. Dong, X.Q. Lai, K.J. Lin, Angew. Chem., Int. Ed. Engl. 36 (1997) 2002.
[8] R.J. Webb, T.-Y. Dong, C.G. Pierpont, S.R. Boone, R.K. Chadka, D.N. Hendrickson, J. Am. Chem. Soc. 113 (1991) 4806.
[9] T.-Y. Dong, P.J. Lin, K.J. Lin, Inorg. Chem. 35 (1996) 6037.
[10] M.D. Rausch, J. Org. Chem. 26 (1961) 1802.
[11] T.-Y. Dong, C.C. Schei, T.L. Hsu, S.L. Lee, S.J. Li, Inorg. Chem. 30 (1991) 2457.